

Improved Mapping of RFID Tags by Fusion with Spatial Structure

Karsten Rohweder Philipp Vorst Andreas Zell

Computer Science Department, University of Tübingen, Tübingen, Germany

Abstract—This paper shows how to exploit knowledge about the spatial structure of an environment in order to obtain more accurate position estimates of passive RFID tags. Such labels are increasingly used as electronic product codes and are originally aimed at identifying goods. Estimating the positions of labeled products, however, is difficult because passive tags only reveal their presence and neither bearings nor distances to them. Previous related work showed that tag detection rates yield decent tag position estimates. Our method combines these solely RFID-based methods with structural information. Indoor experiments with a mobile robot show increased accuracy as compared to mapping purely based on RFID measurements.

Index Terms—Radio frequency identification (RFID); mobile robot; mapping; spatial structure

I. INTRODUCTION

Mobile robots have the potential to become valuable assistants of humans in commercial environments such as supermarkets, warehouses, and logistics buildings. These surroundings have in common that radio frequency identification (RFID) plays an increasingly important role in the labeling of assets, pallets, and products. Each item is given an electronic barcode (called tag or transponder) with a unique identifier. Such tags enable RFID readers to detect objects in a contactless fashion and even without the requirement of line of sight. Moreover, a mobile robot with an on-board RFID reader is able to detect and localize objects without a computationally expensive vision system. This comes, however, at the expense that RFID readers of the prevailing UHF RFID standard (EPC Class 1 Gen. 2) can only detect the presence of a transponder; neither can they determine bearing nor distance to a tag. Even worse, due to read ranges of several meters, a single tag detection yields only a very coarse guess of where the tagged object is located. Several related works have shown, however, that tag position estimation is feasible at a granularity far better than just the technical read range [1, 6, 13]. They achieve this through a number of factors:

- Repeated measurements from various positions and with different orientations of the robot
- Several antennas which point towards different sides of the robot
- Probabilistic sensor models which reflect the correlation between detection rates and the relative displacement and angle between transponder and reader antenna

The third factor, the sensor model, plays a major role. But the currently reported achieved accuracies in estimating the positions of transponders (roughly in the range of 0.4-1.0m, depending on the setup) indicate that too many parameters

have an influence on the actual outcomes of read attempts. Some factors can be taken into consideration easily (e.g., distance and angle between the antenna of the RFID reader and a tag), while others are hard to model (e.g., reflection and absorption caused by equipment and close objects, or multi-path signal propagation).

That is why in this paper we investigate the fusion of RFID measurements with sensors which provide accurate geometric information without disclosing the identity of the scanned structure. We propose a generic approach which is not limited to a specific type of sensor. The reconstruction of spatial structure is decoupled from the mapping stage with RFID data and performed offline beforehand. We employ a probabilistic framework as in related works and integrate spatial structure by the initialization of the estimation process.

This paper is organized as follows: In Sect. II, we present a survey of related work, before we present the tag position estimation approach in Sect. III. Experimental results are provided in Sect. IV, and we finally conclude in Sect. V.



Fig. 1. The mobile platform (RWI B21) with on-board UHF RFID reader, RFID antennas (white), and laser scanner (behind lower antenna) for self-localization. Passive RFID tags were used that were attached to the product packages in the shelf as well as to furniture and walls.

II. RELATED WORK

Hähnel *et al.* were the first to perform RFID-based mapping with particle filters [6]. They employed a laser-based SLAM (simultaneous localization and mapping) algorithm to first determine the trajectory of their robot. Given this trajectory, the positions of passive UHF RFID tags in an indoor environment were estimated, given a probabilistic sensor model of the RFID

reader. Based on the derived map of transponders, the robot localized itself with RFID and odometry alone. In this paper, we build on their probabilistic mapping technique. A variant of Hähnel’s approach is the one by Milella *et al.* [13], in which a fuzzy instead of a probabilistic sensor model is learned. Similarly to Hähnel *et al.*, Deyle *et al.* determined the positions of UHF RFID tags with a particle filter [1]. Their sensor model was fitted to the specified antenna characteristics and included multi-path propagation. Recently, Joho *et al.* [7] combined pure RFID tag detections and signal strength measurements for localization and mapping. They used an RFID-equipped shopping cart in a similar setup as Hähnel *et al.* Their method is also able to iteratively improve the sensor model from a coarse initial model while mapping transponder positions. Moreover, Liu *et al.* [12] performed a variant of Markov localization for tagged objects with an UHF reader. They could also detect if a transponder had moved. A fusion of RFID and stereovision for transponder mapping was proposed by Zhou *et al.* [18]. They used special transponders which had to be activated via a single laser beam.

Kleiner *et al.* [10, 11] showed how to map the locations of sparsely distributed passive short-range tags. They optimize a graph of tag positions whose edges consist of distances estimated via dead-reckoning. The approach expects tags to lie on the floor and relies on the direct proximity to a tag (and thus high certainty in the relative position between the robot and the tag). It has the advantage that it can be pursued by multi-robot teams in a distributed fashion. Tanaka’s work [16] has a similar setup, but uses a recent stochastic gradient descent framework [5, 14] to optimize the constraints given by movements and RFID measurements.

Kantor *et al.* [8] and Djughash *et al.* [2] utilized an extended Kalman filter for localization, mapping and SLAM with active RFID tags. Their methods exploit measured signal strength between the transponders, which is not a standardized feature in passive RFID systems. Kim *et al.* also suggested to evaluate signal strength, but for two perpendicular antennas [9]. This configuration allowed them to estimate the direction of arrival and guide a robot in target docking.

Similar to our approach, Schulz *et al.* combined different types of sensors to track people indoors [15]. They fused the observations of several statically mounted laser range finders, ultrasonic receivers and ID-coding infrared badges in a Rao-Blackwellized particle filter. Our method differs in that the more or less static positions of RFID tags in our setup do not allow for sampling from trajectories and ID associations. Further, we use a mobile platform with just one laser scanner and two pairs of multistatic RFID antennas.

III. TAG POSITION ESTIMATION

A. Overview of our Approach

The fusion approach presented in this paper is motivated by the fact that the position of an RFID tag is coupled with the position of some object to which it is attached. That is, transponders always belong to some spatial structure. This structure can be detected by other sensors than RFID readers like monocular/stereoscopic/depth cameras, 2D/3D laser

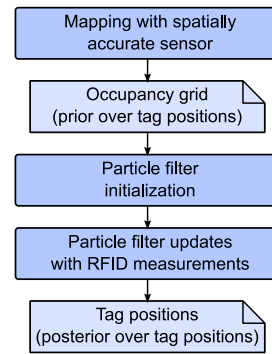


Fig. 2. Overview of the fusion stages

scanners, and ultrasonic or infrared sensors. Combining such a sensor with RFID exploits the geometric accuracy of the former with the identification mechanism of the latter.

The approach presented here is generic insofar as we decouple the spatial reconstruction from the stage of tag position estimation. Thus, various types of sensors can be employed to gain a-priori knowledge about the structure of the environment. In this paper, we use a 2D laser range finder. Our approach also applies to 3D, although there computations are more expensive due to the increased dimensionality.

As shown in Figure 2, a spatial model of the environment is derived first, stored in an occupancy grid. Since the spatial model represents a prior distribution over possible tag locations, it is used to initialize a particle filter. This second stage effectively focuses the particle positions on the areas of interest. Afterwards, the RFID measurements are evaluated, which finally results in a map of transponder positions.

B. Spatial Reconstruction and Representation

The first step of our approach is to generate an occupancy grid map from the readings of a spatially accurate sensor. By accurate, we mean estimation errors of, for instance, few centimeters, but certainly far below the granularity of the RFID reader. An occupancy grid divides the space into an array of grid cells, where each cell denotes the probability of an associated volume of space to contain solid matter. Note that most spatially accurate sensors can yield maps in the shape of occupancy grids: Both for laser-based and (stereo-) vision-based mapping approaches, grid maps can be obtained by registering features. Given the pose of the robot in a global coordinate frame, ray-tracing to observed contours in order to reweight free space and occupied cells. Here, we act on the assumption of dense reconstructions. Assuming that RFID tags only appear where there are objects to carry them, an occupancy grid can be regarded as a natural prior distribution (up to normalization such that all grid cells sum up to one) of where to search the state space of tag positions. This prior distribution is used to initialize a particle filter for tag mapping in order to achieve the desired fusion with RFID, as described subsequently. Ideally, such a grid already exists for self-localization purposes, which means that the grid comes for free for mapping RFID tags.

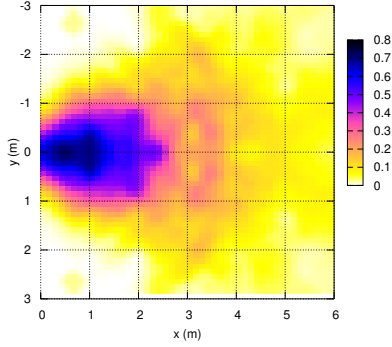


Fig. 3. RFID observation model: Detection rates depend on the relative displacement (here only x, y coordinates) of a tag with respect to the antenna of the RFID reader. The latter is located in the origin and points to the right.

C. Mapping of RFID Tags

In order to map the positions of RFID tags, the robot traverses the environment while its RFID reader is attempting to detect transponders. By using more than one antenna, the robot is able to scan for tags in different directions. At a frequency of 1-2 Hz, the reader reports which tags have recently been detected by which of the antennas. So, formally, at each time step t , a tag is either detected ($d_t^{(k)} = 1$) or not detected ($d_t^{(k)} = 0$) by antenna k . To estimate the position of an RFID tag, we employ particle filtering [3], following the approach by Hähnel *et al.* [6]. A particle filter approximates an arbitrarily shaped probability distribution over the space of possible tag locations by a discrete set of n samples called particles. Each particle consists of a two-dimensional position hypothesis $\mathbf{x}^{(i)} = (x^{(i)}, y^{(i)})$ in world coordinates and a weight $w_t^{(i)}$. Each tag l is associated a separate particle filter.

The particle filter can be initialized by distributing all particles over the detection area of the RFID antenna with which a tag is detected first. This was also Hähnel’s strategy. Our alternative approach integrating knowledge of the spatial structure of the environment will be described in Sect. III-D. Once initialized, the particles are reweighted whenever RFID data arrive:

$$w_t^{(i)} = \eta_t \cdot w_{t-1}^{(i)} \cdot p(d_t^{(k)} | \mathbf{x}^{(i)}, \mathbf{a}_t^{(k)}) \quad (1)$$

$p(d_t^{(k)} | \mathbf{x}^{(i)}, \mathbf{a}_t^{(k)})$ is the observation model and models the likelihood of measuring an RFID tag $d_t^{(k)}$ times, given the static sample position $\mathbf{x}^{(i)}$ and the position $\mathbf{a}_t^{(k)}$ of RFID antenna k . η_t is a normalizer, ensuring that $\sum_{i=1}^n w_t^{(i)} = 1$. The antenna pose $\mathbf{a}_t^{(k)}$ is derived from the current pose estimate of the robot against the map from Sect. III-B. The likelihood function $p(d_t^{(k)} | \mathbf{x}^{(i)}, \mathbf{a}_t^{(k)})$ is learned beforehand, as described in [17]. Figure 3 illustrates the observation model which we used for this work. Note that we also observed that particles should only be reweighted when a tag is detected, i.e., if $d_t^{(k)} = 1$ for some antenna k . Furthermore, we neither perform resampling nor integrate particle motion – which are common particle filtering steps –, because we treat the static case that a tag does not move. The final position estimate of a tag is the weighted mean of its particle positions.

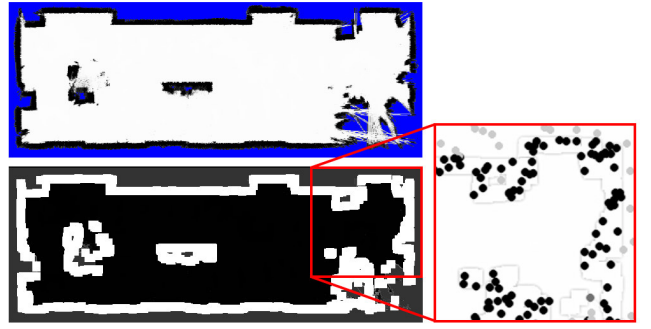


Fig. 4. Illustration of our structural initialization approach. *Upper left*: The occupancy grid representing spatial structure. *Lower left*: Contour detection for the optional case that tags are expected to lie on the outer side of objects. *Right*: Close-up of the map, showing a random initial assignment of particles to occupied cells. Particles are represented by the small circles, where darkness corresponds to weights.

D. Fusing Spatial Structure and RFID Detections by Structural Initialization

The main idea of our approach consists in using the probability of spatial occupation, stored in an occupancy grid, to steer the initial distribution and initial relative weighting of the random samples in the particle filter. In a preprocessing step, contour detection can optionally be performed on the occupancy grid, and the grid cells are reweighted if one favors object contours over solid mass. Contour detection is valuable if tags are expected not to be hidden deeply inside matter. The resulting contour thickness is adjustable to compensate for noise in the chosen spatial reconstruction method. Finally, the particle filter initialization is realized by sampling from the occupancy grid according to distance to a detection position and relative occupancy probability. Particles are then randomly placed in the drawn cells.

Our approach is designed as an offline method which operates on a set of previously recorded position-annotated RFID measurements, but the method is applicable to real-time online processing as well. The following paragraphs will describe first the contour detection and reweighting algorithm, then the occupancy grid cell selection mechanism.

1) *Contour Detection (optional)*: To extract the object contours from the occupancy grid, we first determine the set of cells whose occupancy probabilities fall below a threshold p_{empty} and are thus considered empty, but have non-empty neighbors. For these cells, the magnitude of the occupancy gradient is computed and stored separately. Then, we reweight the occupancy grid in a partitioning process as follows:

- Cells with a probability of less than p_{empty} are left unmodified.
- Centered on cells with a gradient magnitude greater than a threshold g_{thres} , a circular *splat* is painted with a radius of the contour strength and a probability of $p_{contour} = 1.0$.

2) *Cell Selection and Particle Filter Initialization*: The structural information is then used to initialize the particle filter with an a-priori probability distribution in a two-staged process by creating a set of state particles, each representing a weighted hypothesis for a tag position.

First, we collect the set of antenna poses for which a particular tag has been detected. For each of the antenna poses, we then select the subset of cells \hat{C} which are sufficiently close to the antenna pose to be in RFID read range. From these cells, a smaller subset $\bar{C} \subset \hat{C}$ is selected by culling those cells whose weights fall below a threshold; only cells containing structure or structure contours remain in \bar{C} . Normalizing the cell weights in \bar{C} yields the final set of candidate cells C so that $\sum_{c \in C} w_c = 1$.

The set of cells C forms the basis for the sampling stage (detailed in Fig. 5). It generates random tag position hypotheses, constituting the a-priori probability distribution. Our approach sets up a sampling urn U from which cells are drawn with uniform distribution, where individual cell probabilities are given by their relative quantities. While this method does not exactly reproduce the probability distribution of the grid cells, the maximum approximation error ϵ can be chosen arbitrarily small. The advantage of this approach lies in its algorithmic simplicity and favorable time complexity of $\mathcal{O}(kn+m)$, where $n = |C|$ is the number of cells, m the number of particles and k is controlled through the approximation quality ϵ (see Fig. 5). For a maximum error threshold of $\epsilon = 0.05$, usually $k \leq 3$ holds, and other constant factors are low as well. In practice, processing 10 minutes of RFID detections of a tag with 1000 particles incl. structural initialization takes less than 0.1 s on a 3 GHz PC.

For each sampled cell, a tag position hypothesis is created, weighted with the cell's occupancy probability, and added to the particle filter. Upon completion of the random sampling algorithm for each antenna pose, the particle filter is initialized. Particle densities are then such that structure contours are densely populated, structure interiors less so, and overlapping detection areas from different detection positions again densely populated, but proportional to their occupancy probability. This allows for a fine-grained evaluation of the sensor model in the areas that conceivably matter most. The described procedure is illustrated in Fig. 4.

By comparison, without prior knowledge about spatial structure the particles are spread uniformly over a circle around the position of the antenna which first observes the tag (as in [6]). The circle has a radius of the reader's read range.

E. Structural Initialization vs. Subsequent Fusion

Another straightforward way of fusing RFID measurements with structural data would be to integrate the structural knowledge only *after* evaluating all RFID inquiries. This procedure would also potentially allow for interleaving structural mapping, based on a camera or a laser range finder, with the localization of the transponders. Assuming the independence of RFID measurements and structural mapping, the final weight of the i -th particle in this alternative approach would be:

$$w_{final}^{(i)} = \eta \cdot w_t^{(i)} \cdot p_{occupied}(\mathbf{x}^{(i)}) \quad (2)$$

Thereby, η is again a normalizer, t is the final time step, and $p_{occupied}(\mathbf{x}^{(i)})$ is the occupancy probability at the particle's position. Visually, this method constrains the sample set to occupied positions of the occupancy grid; the weights of

Input: Set of normalized candidate cells C with cardinal number $n = |C|$, number of particles m , threshold ϵ of the accumulated error, partially initialized or uninitialized particle filter P

Output: Initialized particle filter P

```

 $D \leftarrow \emptyset$  // set of cells and their counts
 $c_{min} \leftarrow \min(c \in C)$  // least cell weight
 $w_{mult} \leftarrow 0$  // granularity control factor

// Refine cell counts while error exceeds threshold:
repeat
   $\eta \leftarrow 0$  // accumulated error
   $w_{mult} \leftarrow w_{mult} + 1$ 
  // Create cell counts  $d$ :
  forall  $c \in C$  do
     $d \leftarrow \lceil c \cdot \frac{w_{mult}}{c_{min}} \rceil$ 
     $D \leftarrow D \cup \{(c, d)\}$ 
  end
  // Summarize deviation of approximated cell probabilities
  from true random distribution:
  forall  $(c, d) \in D$  do
     $p_{approx} \leftarrow d \cdot \left(\sum_{d_i \in D} d_i\right)^{-1}$ 
     $p_{true} \leftarrow c$ 
     $\eta \leftarrow \eta + |p_{approx} - p_{true}|$ 
  end
until  $\eta \leq \epsilon$ ;

// Create urn to draw from:
 $U \leftarrow \emptyset$ 
forall  $(c, d) \in D$  do
  for  $i \leftarrow 1$  to  $d$  do
     $U \leftarrow U \cup \{(c, i)\}$ 
  end
end

// Initialize particle filter:
for  $i \leftarrow 1$  to  $m$  do
   $(c_r, d) \leftarrow$  draw from  $U$  using uniform distribution
   $p \leftarrow$  create particle which lies in  $c_r$  (i.e.,  $\mathbf{x}^{(i)} \in c_r$ )
   $P \leftarrow P \cup \{p\}$ 
end

```

Fig. 5. Sampling algorithm for distributing the tag location particles to occupancy grid cells.

particles with implausible positions will be decreased or even set zero if particles lie on free space.

IV. EXPERIMENTS

A. Setup

In order to measure the accuracy of our fusion approach, we conducted several indoor experiments with an RWI B21 robot (Fig. 1 on p. 1). The robot is equipped with a laser range finder (240° field of view) for accurate positioning. The on-board RFID reader is an Alien technology ALR-8780 UHF reader with two pairs of multistatic antennas. They point at angles of approx. 45° sideways. Each antenna pair detects tags with rates as depicted in Fig. 3. The experimental environment was a laboratory with a free space of approx. 50 m². More than 400 passive UHF tags at different heights and orientations were attached to walls, furniture, and empty product packages in a metal shelf. We recorded 34 datasets on manually steered, arbitrary paths through the lab. In the scope of the experiments

the robot traveled a distance of 3.0 km over a duration of 3.9 h. Approximately 20,000 RFID readings were performed. Additionally, we built a 2D laser occupancy grid of the lab, using the laser-based grid SLAM module GMapping [4]. During mapping, the position of the robot was then estimated via the laser scanner.

On these datasets, we compared the performances of the three mapping techniques: a particle filter which is initialized uniformly and does not take spatial knowledge into account (subsequently referred to by “UNI”); the particle filter which is initialized with structural knowledge (“STR”) as described in Sect. III-D; and a particle filter with uniform initialization, but fusion with spatial knowledge after the evaluation of all RFID measurements (“SUB”) as described in Sect. III-E.

B. Mapping Accuracy

For a particle filter with 1000 particles, we compared the mean absolute errors of tag position estimates for the three mapping techniques. The comparison is based on 40 transponders, whose true positions were determined manually. These tags were located both on the exteriors of objects and inside shelves, and their heights varied from 0.28 m to 1.38 m over ground. For each dataset, the particle filter was run ten times to meet its random nature. The results are shown in Table I. A mean error of approx. 0.95 m was obtained for the standard approach without fusion (UNI). Integrating knowledge about structure by the initialization strategy (STR) reduced the error to approx. 0.86 m. This is an improvement of 9.7%. The subsequent fusion with spatial knowledge (SUB) also reduced the error, but only by 3.3% to a value of 0.93 m. The improvements show that taking knowledge about spatial structure into account is beneficial with regard to lower mapping errors. An example mapping result is illustrated in Fig. 6.

A useful measure for assessing why the initialization approach performs better than the subsequent fusion with occupancy information is the *effective sample size* (ESS) [3]. The ESS reveals the degeneracy of a particle filter and indicates how many particles have non-negligible weights. Note that by iteratively applying the sensor model as described above, many particles will have weights close to zero. We computed the estimate of the ESS relatively to the size of the sample set: $\hat{N}_{eff,rel} = n^{-1} / \sum_{i=1}^n (w_t^{(i)})^2$. The first insight given by

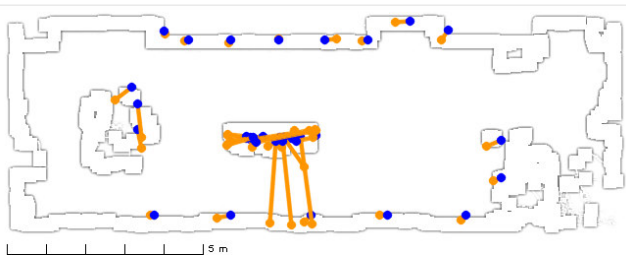


Fig. 6. Example of a generated map with tag position estimates (orange/light gray dots) and associated ground truth (blue/black dots). Most tag positions were estimated accurately. Larger errors occur where metallic reflections at radiators frequently yielded ghost detections of tags (bottom part of the image).

TABLE I
RESULTS OF UNIFORM AND STRUCTURAL INITIALIZATION: MEAN ABSOLUTE MAPPING ERRORS AND MEAN EFFECTIVE SAMPLE SIZE RELATIVE TO THE SIZE OF THE PARTICLE FILTER (ESS)

Initialization	Mean error \pm Std. dev. (m)	ESS (%)
UNI (no fusion)	0.9497 \pm 0.1464	0.95
STR (fusion by initializ.)	0.8579 \pm 0.1703	1.32
SUB (subsequent fusion)	0.9275 \pm 0.1733	0.43

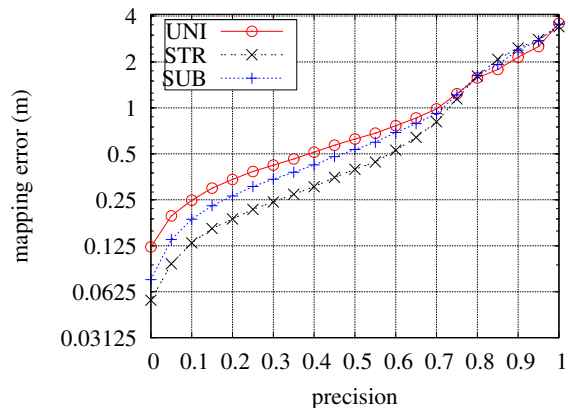


Fig. 7. Accuracy vs. precision: The x -axis denotes the fraction of tags that have a mean mapping error of less than the value on the (logarithmic) y -axis.

Table I is that many particles (more than 98%) hardly contribute to the position estimate. This, however, is an inherent difficulty of mapping the positions of UHF RFID tags: The uncertainty of RFID measurements is large, because RFID readers feature read ranges of several meters. The second insight is that by initializing the particles to occupied positions, more particles effectively contribute to the position estimates: almost 40% more (STR) than in the case of the uninformed initialization (UNI). That is, using the occupancy grid as a proposal distribution, the samples are guided to regions of higher likelihood. The subsequent fusion (SUB), by contrast, improves the position estimate, but at the cost of an even smaller ESS. This effect is plausible, because applying Eq. 2 naturally leads to a larger variance of particle weights. Because of these insights, we increased the number of particles. Even with 10,000 samples, however, the uniform initialization did not yield better results.

Figure 7 illustrates the mapping error, averaged over all experiments, for different fractions of investigated tags. For the best 75% of the tag estimates, the fusion approaches yield better results. The structural initialization (STR) roughly halves the error for the best third of the estimates. Rather surprising at first glance is the outcome that the worst 20% of the tag estimates are better if no fusion takes place. The example in Fig. 6, however, indicates that the effect is caused by outliers: Structural initialization can place particles on even more unlikely positions in case of outliers. Indeed, outlier rejection should deserve further attention in RFID-based mapping, but is beyond the scope of this work.

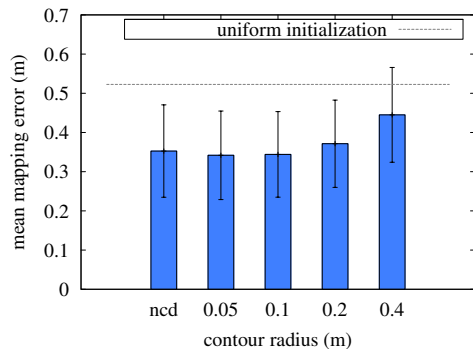


Fig. 8. Mean errors and standard deviations of tag position estimates for different contour radii (see Sect. III-D), compared to a uniform initialization of particles without spatial knowledge. “ncd” means that contour detection was not performed.

C. Tags on Exteriors of Objects

Typically, tags will be attached to the exteriors of objects. If the special case holds that objects are not placed one after another and transponders are not hidden deeply inside matter, our fusion approach can utilize these conditions. A typical scenario in which this special case holds is when RFID tags are used as manually installed navigation stimuli, e.g., attached to walls as artificial landmarks.

Figure 8 shows the results which we obtained for this special case, using 1000 particles. The evaluation is based on 15 tags, attached to walls roughly at the height of the upper RFID antennas. The mean estimation error was reduced to approx. 0.35 m in this case. This is an improvement of about 33 %, as compared to 0.52 m without fusion.

V. CONCLUSION

In this paper, we presented a fusion approach to the mapping of passive UHF RFID transponders with a mobile robot. It exploits the fact that tags are attached to objects and therefore coupled with matter. The spatial knowledge is utilized as an a-priori probability distribution over the space of possible transponder locations and extends the particle filter-based methods by Hähnel *et al.* [6]. The approach is generic insofar as any kind of spatially sufficiently accurate, commonly used sensor (e.g., laser scanner or camera) can be employed for acquiring a spatial model of the environment.

Considering the two-dimensional case with a 2D RFID sensor model and a 2D laser range finder, our experiments showed significant reductions of estimation errors: The mean error of approx. 0.85 m on a mixed set of transponders represents an improvement of approx. 10 %. For the special case of RFID tags as artificial landmarks, the estimation error even decreased by one third, from 0.52 m to 0.35 m. These improvements justify the extra efforts of the fusion: In robotic inventory, for instance, one will be interested in positions estimates which are as accurate as possible.

Future work will comprise the detection of outliers in RFID measurements, encountering the problem of electromagnetic reflections. The extension of our approach to three dimensions is promising, too. In order to improve mapping accuracy by means of cameras, one could additionally integrate information

such as color or texture to recognize objects (e.g., product packages) within line of sight.

ACKNOWLEDGMENT

This paper was funded by the Landesstiftung Baden-Württemberg in the scope of the BW-FIT project AmbiSense.

REFERENCES

- [1] T. Deyle, C. Kemp, and M. Reynolds. Probabilistic UHF RFID tag pose estimation with multiple antennas and a multipath RF propagation model. In *Proc. of the 2008 IEEE/RSJ Int. Conference on Intelligent Robots and Systems (IROS)*, pages 1379–1384, Nice, France, 2008.
- [2] J. Djughash, S. Singh, and P. Corke. Further results with localization and mapping using range from radio. In *International Conference on Field and Service Robotics (FSR)*, volume 25 of *Springer Tracts in Advanced Robotics*, pages 231–242, 2005.
- [3] A. Doucet, S. Godsill, and C. Andrieu. On sequential Monte Carlo sampling methods for Bayesian filtering. *Statistics and Computing*, 10:197–208, 2000.
- [4] G. Grisetti, C. Stachniss, and W. Burgard. Improving grid-based SLAM with Rao-Blackwellized particle filters by adaptive proposals and selective resampling. In *Proc. of the IEEE International Conference on Robotics & Automation (ICRA)*, 2005.
- [5] G. Grisetti, C. Stachniss, S. Grzonka, and W. Burgard. A tree parameterization for efficiently computing maximum likelihood maps using gradient descent. In *Robotics: Science and Systems III*, Atlanta, GA, USA, 2007.
- [6] D. Hähnel, W. Burgard, D. Fox, K. Fishkin, and M. Philipose. Mapping and localization with RFID technology. In *Proc. of the 2004 IEEE International Conference on Robotics and Automation (ICRA)*, pages 1015–1020, 2004.
- [7] D. Joho, C. Plagemann, and W. Burgard. Modeling RFID signal strength and tag detection for localization and mapping. In *Proc. of the IEEE International Conference on Robotics and Automation (ICRA)*, Kobe, Japan, 2009.
- [8] G. Kantor and S. Singh. Preliminary results in range-only localization and mapping. In *Proc. of the IEEE Conference on Robotics and Automation (ICRA)*, May 2002.
- [9] M. Kim, N. Chong, and W. Yu. Robust DOA estimation and target docking for mobile robots. *Intelligent Service Robotics*, 2(1):41–51, January 2009.
- [10] A. Kleiner, C. Dornhege, and S. Dali. Mapping disaster areas jointly: RFID-coordinated SLAM by humans and robots. In *Proc. of the IEEE Int. Workshop on Safety, Security and Rescue Robotics (SSRR)*, Rome, Italy, 2007.
- [11] A. Kleiner, J. Prediger, and B. Nebel. RFID technology-based exploration and SLAM for search and rescue. In *Proc. of the IEEE/RSJ International Conference on Intelligent Robots and Systems (IROS)*, Beijing, China, pages 4054–4059, 2006.
- [12] X. Liu, M. Corner, and P. Shenoy. Ferret: RFID localization for pervasive multimedia. In *Proc. of Ubicomp*, Irvine, CA, September 2006.
- [13] A. Milella, P. Vanadia, G. Cicirelli, and A. Distante. RFID-based environment mapping for autonomous mobile robot applications. In *IEEE/ASME International Conference on Advanced Intelligent Mechatronics*, pages 1–6, Zürich, Switzerland, 2007.
- [14] E. Olson, J. Leonard, and S. Teller. Fast iterative optimization of pose graphs with poor initial estimates. In *Proc. of the IEEE International Conference on Robotics and Automation (ICRA)*, pages 2262–2269, 2006.
- [15] D. Schulz, D. Fox, and J. Hightower. People tracking with anonymous and ID-sensors using Rao-Blackwellised particle filters. In *Proc. of the International Joint Conference on Artificial Intelligence (IJCAI)*, Acapulco, Mexico, 2003.
- [16] K. Tanaka. Multiscan-based map optimizer for RFID map-building with low-accuracy measurements. In *Proc. of the 19th International Conference on Pattern Recognition (ICPR)*, pages 1–4, 2008.
- [17] P. Vorst and A. Zell. *European Robotics Symposium 2008*, volume 44/2008 of *Springer Tracts in Advanced Robotics*, chapter Semi-Autonomous Learning of an RFID Sensor Model for Mobile Robot Self-localization, pages 273–282. Springer, 2008.
- [18] Y. Zhou, W. Lu, and P. Huang. Laser-activated RFID-based indoor localization system for mobile robots. In *Proc. of the IEEE International Conference on Robotics and Automation (ICRA)*, pages 4600–4605, Rome, Italy, April 2007.